Chemical Engineering Journal 158 (2010) 167–172

Contents lists available at ScienceDirect

Chemical Engineering Journal

journal homepage: www.elsevier.com/locate/cej

Cr-doped titanite pigment based on industrial rejects

W. Hajjaji [a], C. Zanelli [b], M.P. Seabra [a], M. Dondi [b], J.A. Labrincha [a,*]

[a] Ceramics and Glass Engineering Department, CICECO, University of Aveiro, 3810-193 Aveiro, Portugal
[b] Istituto di Scienza e Tecnologia dei Materiali Ceramici, CNR-ISTEC, 48018 Faenza, Italy

ARTICLE INFO

Article history:
Received 30 October 2009
Received in revised form
11 December 2009
Accepted 16 December 2009

Keywords:
Chromium doping
Titanite
Ceramic pigment
Marble sawing sludge
Galvanizing waste
Foundry sand

ABSTRACT

This work reports the development of inorganic pigments based on chromium doped titanite ($CaTiSiO_5$). For economical and environmental reasons, wastes were used as raw materials but similar formulations from pure reagents were also prepared to assess the effect of impurities contained in wastes. Pigments were characterised by XRD, SEM + EDS microprobe analysis, and UV–vis–NIR spectroscopy. The colouring mechanism (the pigment is reddish brown) seems to result from the combined contribution of octahedral Cr(III) and tetrahedral Cr(IV) species replacing Ti^{4+} and Si^{4+}, respectively. In both pure reagents and waste-based pigments, colorimetric parameters were evaluated and their colouring performance was tested in transparent and opaque ceramic glazes. Intense and stable brown hues were developed with optimized formulations, i.e. containing 0.044Cr at 1300 °C.

1. Introduction

The current work describes brown Cr-doped sphene pigments, formed by the solid-state reaction method from either pure reagents or industrial wastes. Contrarily to Cr-doped malayaite ($CaSnSiO_5$), widely studied and used to colour ceramic products thanks to its characteristic pink hue [1–4], its titanium analogue (titanite) is less common in such applications [5,6]. Titanite is a nesosilicate that crystallises in the monoclinic system [7–9], space group $P2_1/a$, with a high temperature polymorph isostructural to malayaite (space group $A12/a1$). Titanium ions are located in octahedral positions; silicon is in tetrahedral coordination while Ca^{2+} occupies an irregular seven-coordinated site [5–10]. The titanite framework is composed of octahedra linked by vertexes to form chains, which are cross-linked by adjacent SiO_4 tetrahedra. In this array, the average bond strength in O(2), O(3), O(4) and O(5) sites reaches 2 due to the occupancy by oxygen shared with tetrahedral Si. Only the O(1) atom is linked exclusively to Ti forming an octahedral chain of Ti–O(1). This configuration allows substitution in this site by M^{4+} cations [11,12], as Cr^{4+} along with Cr^{3+}, in a similar way to that found for malayaite [4,13]. The incorporation of metal ions is known in both natural and synthetic titanite samples and was reported in several works [8,14].

Cr-doped titanite pigments can be looked as a good solution to replace other brown pigments, currently used in ceramic manufacturing, like $(Fe,Mn)(Fe,Mn,Cr)_2O_4$ (DCMA 13-48-7), $(Zn,Mn)(Mn,Cr)_2O_4$ (DCMA 13-51-7) and $NiFe_2O_4$ (DCMA 13-35-7) spinels, or doped rutile $(Ti,Nb,Mn)O_2$ (DCMA 11-47-7) with avoiding instable (Mn) or toxic (Ni). In addition, the interest to develop low cost titanite pigments is increased by using wastes instead of pure reagents. If properly selected, they can assure the correct colour and may decrease the sintering temperature and the overall costs. The approach of using wastes, like those from Cr/Ni plating, marble cutting and foundry moulds, as sources of chromium, calcium and silicon, respectively, is supported by other recent promising industrial and environmental investigations done to produce pink malayaite [3].

2. Materials and synthesis procedure

The sol–gel and solid-state reaction method are the main used processing routes to synthesize ceramic pigments. The first one involves the use of suitable liquid precursors and assures a better control of grain size distribution and of the structural stoichiometry of the processed formulations. Vanadium–zircon blue or uvarovite victoria green pigments are normally obtained by this method [15–17]. As main drawback the processing costs are higher than in the conventional solid-state reaction method, even if this last route requires the use of relatively high sintering temperatures to form stable structures. The ceramic route is then more simple and easy to implement at an industrial level. It involves the main following steps: mixing/milling of reagents; calcination of powders; dry milling and sieving to adjust the grain size [16].

* Corresponding author. Tel.: +351 234370250; fax: +351 234370204.
E-mail address: jal@ua.pt (J.A. Labrincha).

1385-8947/$ – see front matter © 2009 Elsevier B.V. All rights reserved.
doi:10.1016/j.cej.2009.12.026

Table 1
Chemical composition of reagents (determined by XRF or given by the producer) and pigment batch formulations: P = pure reagents and S = sludge containing formulations.

	Calcite (Calcitec)	Marble sludge (MS)	Silica (Sibelco)	Foundry sand (FS)	Cr(III) nitrate (Fluka)	Cr/Ni Sludge (GS)	Rutile (Kronos)
SiO_2	0.10	0.64	99.01	97.62	–	0.17	–
TiO_2	0.01	0.02	0.01	0.20	–	–	99.83
Al_2O_3	0.10	0.14	0.10	0.20	–	0.12	–
Fe_2O_3	0.07	0.24	0.06	1.12	–	0.30	0.03
Cr_2O_3	–	–	–	0.20	37.50	17.40	–
MgO	0.20	0.31	0.07	–	–	0.32	–
CaO	55.60	55.54	0.10	0.20	–	12.60	–
NiO	–	–	–	–	–	25.10	–
CuO	–	–	–	–	–	15.18	–
ZnO	–	–	–	–	–	0.06	–
Na_2O	0.01	–	0.05	–	–	1.09	–
K_2O	0.01	0.11	0.10	0.26	–	0.03	–
P_2O_5	–	–	–	–	–	9.85	0.02
SO_3	–	–	–	–	–	2.29	0.02
LOI	43.9	43.00	0.50	0.20	–	15.59	0.10
P–0.024Cr/Ti	40.4	–	24.2	–	3.9	–	31.5
S–0.024Cr/Ti	–	36.9	–	25.7	–	4.4	33.0
P–0.044Cr/Ti	39.4	–	23.6	–	6.9	–	30.1
S–0.044Cr/Ti	–	35.2	–	25.1	–	7.8	31.9
P–0.064Cr/Ti	38.4	–	23.0	–	9.8	–	28.7
S–0.064Cr/Ti	–	33.6	–	24.5	–	11.1	30.8

So in the actual paper the Cr-doped titanite was prepared by the ceramic route. Combinations of pure reagents were designed shifting the ratio Cr/Ti (0.024, 0.044, and 0.064) like expressed in Table 1. Analogous formulations were then prepared by substituting as much as possible pure reagents by secondary raw materials (industrial wastes). The maximum substitution level reached 71 wt.% of the initial batch according to the following scheme: marble sawing sludge (MS), Cr/Ni galvanizing sludge (GS) and foundry sand (FS) instead of calcite (Calcitec), chromium (III) nitrate (Fluka), and silica (Sibelco), respectively. Batch formulations are summarized in Table 1 and were wet-ball milled for 60 min then dried at 100 °C overnight. The calcination cycle (electric kiln) was carried out at 5 °C/min heating and cooling rates and 3 h dwell time at the maximum temperature: 1100, 1200 or 1300 °C. Pigments so obtained were then ball milled, dried and sieved below 63 μm.

Crystalline phases present on fired samples were analysed by X-ray diffraction (Rigaku Geigerflex diffractometer with filtered Cu Kα radiation in 10–80°2θ range, scan rate 0.02°2θ, 4 s per step). The quantitative phase analysis was performed using GSAS-EXPGUI software following a RIR (Reference Intensity Ratio) and the Rietveld refinement techniques [18,19]. Up to 40 independent variables were refined: scale-factors, zero-point, 15 coefficients of the shifted Chebyschev function to fit the background, unit cell dimensions, profile coefficients (1 Gaussian, GW, and 2 Lorentzian terms, LX and LY). The agreement indices, as defined in GSAS, for the final least-squares cycles of all refinements are represented by R_p (%), R_{wp} (%), X^2 and $R(F^2)$ (%).

The analysis was complemented by scanning electron microscopy (SEM, Hitachi, SU 70) with in situ chemical determinations obtained by a microprobe XRF-EDS (Bruker AXS, software: Quantax). The colour of pigments was evaluated by measuring $L^*a^*b^*$ (L^*: 0 = black/100 = white, green ($-a^*$) to red (+a*) and blue ($-b^*$) to yellow ($+b^*$) parameters with a Konica-Minolta Chroma Meter CR-400 [20]. UV–vis–NIR spectra were acquired by absorption spectroscopy (Shimadzu UV-3100, step interval 2 nm) using a $BaSO_4$ standard as white reference material in order to understand the colouring mechanism.

Titanite pigments were used to colour transparent and opaque glazes (1/20 weight ratio), which were fired at 1050 °C (5 °C/min heating and cooling rate and 30 min dwell time). The colour of the glazes was studied by the two last techniques as already described previously for pigments. The possible formation of surface defects (bubbles, cracks, non-homogeneity) was also checked.

3. Results

Pigments obtained from pure reagents show the presence of titanite associated with quartz, cristobalite, wollastonite ($CaSiO_3$) and perovskite ($CaTiO_3$) after calcination at 1100 and 1200 °C (Fig. 1). This assemblage, consistent with the for SiO_2–$CaTiO_3$–$CaTiSiO_5$ sub-system of the SiO_2–CaO–TiO_2 ternary diagram [21] turn into a titanite quasi-single phase at 1300 °C (98.7 wt.%) (Table 2).

Table 2
Phase composition established by Rietveld refinements of pigments.

	P–0.044Cr/Ti_1100	P–0.044Cr/Ti_1200	P–0.044Cr/Ti_1300	S–0.044Cr/Ti_1300
Phase quantification (wt.%)				
Titanite	10.1 (0.1)	49.6 (0.3)	98.7 (0.1)	90.2 (0.1)
Perovskite	49.9 (0.1)	26.9 (0.3)	1.3 (0.1)	–
Wollastonite	19.5 (0.1)	12.0 (0.1)	–	–
Nickel titanate	–	–	–	4.7 (0.3)
Cristobalite	–	4.9 (0.1)	–	5.0 (0.1)
Quartz	20.1 (0.2)	6.6 (0.3)	–	–
Refinement indices				
Rwp (%)	20.6	18.4	23.1	24.5
Rp (%)	15.5	13.7	18.3	18.9
R (B) titanite only (%)	20	13.2	16	19.2
X^2	2.1	1.6	2.4	3.3
$R(F^2)$	20	13.7	15.6	19.5

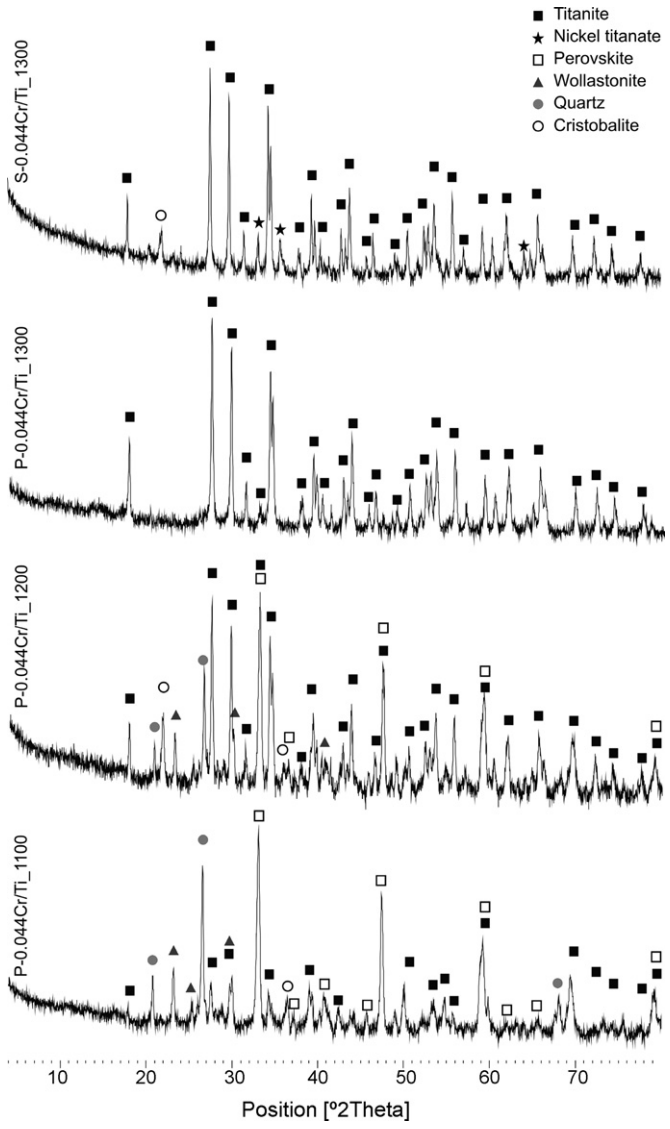

Fig. 1. XRD patterns of sintered Cr-doped titanite formulations: P = pure reagents and S = waste containing.

By using wastes, along with the phase evolution observed starting from pure reagents, a second phase is formed together with titanite (90.2 wt.%) and nickel titanate ($NiTiO_3$: 4.7 wt.%). This results from the occurrence of Ni in the GS sludge that is also the source of chromium. Reaction of nickel with TiO_2 led some free SiO_2 in the final powders.

Table 3
EDS elemental quantification.

	at.%		
	P	S	NT
O	5	5	3
Si	1.000	1.000	0.000
Ti	0.924	0.928	1.104
Cr	0.039	0.026	0.058
Ni	0.000	0.000	0.551
Ca	1.094	1.106	0.153
Total	3.057	3.060	1.866
Ti + Cr	0.962	0.954	–
Cr/Ti	0.042	0.028	–

In situ chemical analyses of samples calcined at 1300 °C (see Table 3) reveal some excess of SiO_2 with respect to the theoretical titanite likely due to some cristobalite contribution. Anyway, constraining the SiO_2 to the value corresponding to the exact occupancy of the tetrahedral site, nearly full occupancy of Ti + Cr in the octahedral site and Ca in the 7-fold coordinated polyhedron are achieved (Table 3). The Cr/Ti ratio in P-0.044Cr/Ti_1300 is equal to the designed value (0.043), while it is slightly lower in particle P (Cr/Ti = 0.028) (Fig. 2 and Table 3). Further EDS analyses of pigments calcined at 1100 or 1200 °C (not shown) reveal particles that seem to have the expected stoichiometry of titanite but without chromium. This suggests that chromium is incorporated into the titanite structure only for temperatures superior to 1200 °C, when the system turns into monophasic, as detected by XRD. In the S-pigment, the additional phase $NiTiO_3$ was identified, even if the composition of this ilmenite-like phase (particle NT, see Fig. 2) seems to contain some Ca and Cr among Ni due to the effect of surrounding titanite that can cause compositional deviations in the punctual analysis (Table 3).

The UV–vis–NIR spectra show important differences between P and S pigments in the visible and NIR regions. The absorbance of the pigment produced from pure reagents is higher in visible range, which should be materialized better colour, while S-pigment absorbs more in NIR and red light (inferior to 600 nm). In same interval, the variation in absorbance (about 17.000 cm^{-1}) could be related to different contribution level of spin-forbidden transitions Cr^{3+} (d^3 electronic configuration) [22–24]. The weak bands individualised in NIR and centred at 1140 nm are consistent with the $^3A_2 \rightarrow {}^3T_2(F)$ transition matched to Cr(IV) species substituting Si(IV) in tetrahedral positions [25–27]. Due to the large disparity of ionic radii between the two species and the need to assure charge

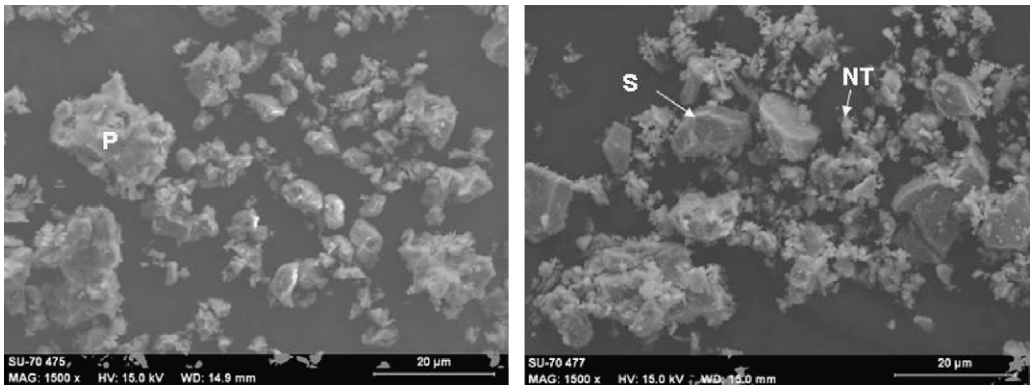

Fig. 2. Microstructure of pigment powders.

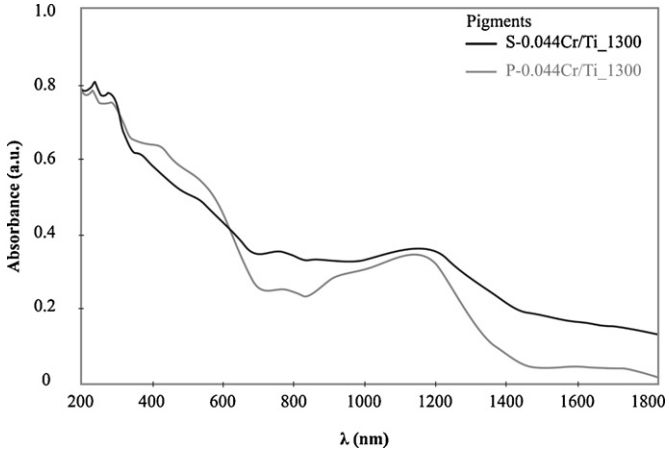

Fig. 3. UV–vis–NIR spectra of pigments.

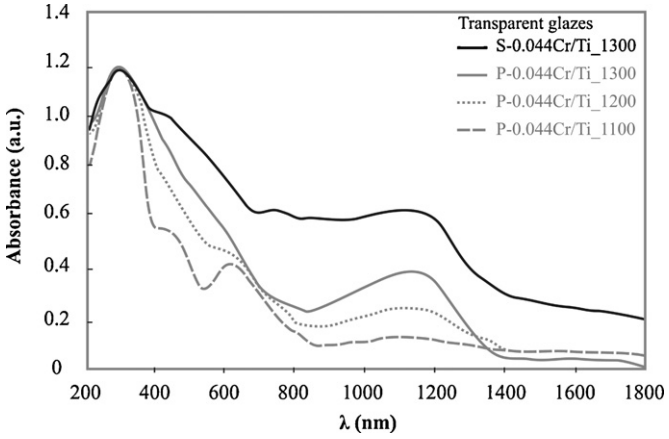

Fig. 4. Absorbance spectra of coloured transparent glazes.

electroneutrality, it is unlikely that octahedral Cr^{3+} species might replace tetrahedral Si^{4+} ions.

Due to extensive overlapping, the ill-resolved optical bands are difficult to be interpreted. The presence of tetravalent chromium excitations in the visible domain, either in octahedral as in tetrahedral coordination, is hindered by superimposed stronger Cr^{3+} transition bands [23].

Nevertheless and from Fig. 3, we can consider a band at 405 nm attributed with $^3A_2 \rightarrow {}^3T_2(P)$ transfer of Cr(IV) [28–30] and a second one is located around 500 nm (≈20.000 cm^{-1}) due to spin-allowed transition of octahedral Cr(III) from $^4A_{2g}$ ground state to the excited $^4T_{1g}(F)$ state [24]. These two sequential absorptions located in the violet (405 nm) and green-blue (500 nm) zones are responsible for the brown colour displayed by the pigment.

The absorbance spectra of chromium-doped titanite containing transparent glazes are shown in Fig. 4. In the near infrared region, the wide band observed at 1140 nm coincides with the emission $^3A_2 \rightarrow {}^3T_2(F)$ of tetrahedral Cr^{4+} species detected in the pigments [27,30]. It is visible the difference in the electronic behaviour between glazes containing pigments calcined at 1300 °C and those coloured by pigments calcined at 1100 and 1200 °C (Fig. 4). This should be related to the level of chromium incorporation in the glassy network that might occur on pigments where the titanite formation was not complete, as previously reported in XRD and SEM/EDS analyses. Glazes containing P-0.044Cr/Ti_1100 and P-0.044Cr/Ti_1200 pigments show a broad emission at about 640 nm that is compatible with the presence of free Cr(III) species and their gradual incorporation in the glassy phase [25]. This band becomes smoother for the pigment calcined at 1200 °C and disappears for pigments fired at 1300 °C.

The only certitude extracted from the analysis of optical spectra of glazes that they are closer to those obtained for the pigments and the mentioned differences in the absorbance spectra between P and S pigments are much lower, confirming the stability of the last at 1300 °C.

Table 4 gives the CIELab colorimetric parameters of the pigments and applications (selected transparent and opaque glazes). The effect of calcination temperature on the colour of P-0.044Cr/Ti pigments is given by a slight decrease of lightness (L^*) and red hue ($+a^*$), while the value of yellow-blue (b) coordinate is constant.

The green hue (Fig. 5) and negative a^* values (Table 4) shown by the glazes coloured by pigments calcined at 1100 and 1200 °C may be attributed to the chromium leaching from the pigments that was then incorporated or dissolved in the glaze matrix. When all chromium is incorporated in the pigment lattice, that seems to occur after calcination at 1300 °C as suggested by XRD and SEM analysis, the colour of the applications change from green to the expected brown.

Differences on colour of the applications achieved by using P or S pigments are noticed by changes in the brown hue (see for example S-0.044Cr/Ti_1200 and P-0.044Cr/Ti_1200). Formulations prepared from wastes have lower red component (Table 4), as a probable effect of the co-existence of phases like $NiTiO_3$. Nevertheless, among the principal component Cr-doped titanite, the impurities introduced by recycling materials seem to enhance the brown coloration in transparent glaze support (Fig. 5). In fact this is reflected by a low lightness such in S-0.044Cr/Ti_1300 and S-0.064Cr/Ti_1300 pigments comparing to P-0.044Cr/Ti_1300 and P-0.064Cr/Ti_1300 obtained from pure reagents.

Further trials conducted to study the effect of changing the Cr/Ti ratio (0.024 and 0.064), reveal the expected tendencies. By lowering the relative amount of chromium, lighter brown coloration was obtained in transparent and opaque glazes, following a similar tendency on the pigments. At the same time, it is easy to see

Table 4
CIELab parameters pigments, transparent and opaque glazes.

Reference	Pigments			Transparent glaze			Opaque glaze		
	L^*	a^*	b^*	L^*	a^*	b^*	L^*	a^*	b^*
P–0.044Cr/Ti_1100	52.7	8.3	9.0	58.2	−8.6	11.4	81.1	−2.0	9.4
S–0.044Cr/Ti_1100	49.7	8.3	9.0	49.1	−4.0	12.0	77.6	−0.8	9.7
P–0.044Cr/Ti_1200	49.7	9.2	9.6	50.3	−0.2	12.0	74.0	2.9	10.3
S–0.044Cr/Ti_1200	50.8	4.8	9.0	43.1	2.0	9.9	72.6	1.6	7.6
P–0.044Cr/Ti_1300	47.5	7.8	9.4	44.2	4.8	11.3	69.3	4.0	8.7
S–0.044Cr/Ti_1300	52.9	4.3	8.9	34.9	3.6	7.1	73.4	1.4	5.3
P–0.024Cr/Ti_1300	59.8	6.7	11.3	46.8	4.6	12.1	75.3	2.7	6.7
S–0.024Cr/Ti_1300	63.7	3.7	11.4	48.1	1.5	11.7	79.2	0.7	8.1
P–0.064Cr/Ti_1300	55.6	7.0	10.5	38.1	4.5	9.5	70.4	3.5	8.7
S–0.064Cr/Ti_1300	54.7	3.1	7.0	37.0	1.3	7.5	72.8	0.7	7.3

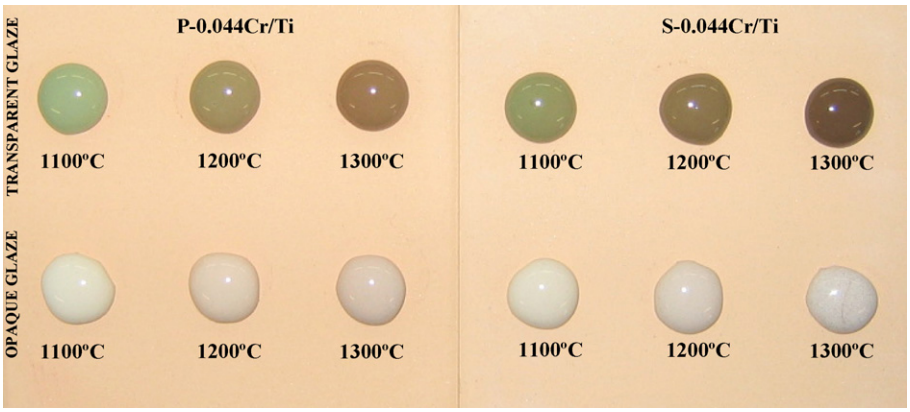

Fig. 5. Colour variation of transparent and opaque glazes containing P-0.044Cr/Ti and S-0.044Cr/Ti pigments (1/20 weight ratio).

that the further increase of chromium concentration (Cr/Ti = 0.064) does not induce significative improvements in the colour performance of pigments in the tested transparent glazes. However, differences between S and P formulations are stronger, since the relative amount of GS sludge is higher. S-0.044Cr/Ti_1300 and P-0.044Cr/Ti_1300 pigments are then considered the optimal formulations. These promising results in transparent glaze are not reflected in the opaque glaze (Fig. 5). The opaque matrixes tend to shade the colour (lightness is over 69.3) so there is a need to increase the added amount of titanite pigment (over 5 wt.%) to equalize the hue intensity achieved by the use of brown spinel or rutile pigments.

4. Conclusions

The mineralogical study of pigments obtained from pure reagents reveal that formation of single titanite phase is completed only after calcination at 1300 °C, being this the recommended sintering temperature. Quartz, cristobalite, wollastonite ($CaSiO_3$) and perovskite ($CaTiO_3$) are unreacted or intermediate phases detected in powders calcined at 1100 and 1200 °C. The presence of impurities in the wastes might contribute to anticipate the sintering process, due to the fluxing characteristics of some of them.

UV–vis–NIR spectra showed two main bands assigned to transitions on octahedral Cr(III) and tetrahedral Cr(IV) species replacing Ti^{4+} and Si^{4+} ions, respectively. The colour changes in the applications, from green to brown, are explained by the reaction level and crystallisation degree of Cr-doped titanite. Waste containing pigments calcined at 1300 °C show $NiTiO_3$ in addition to titanite. That phase might be responsible for the darker brownish hue obtained either in the pigment as in the glazes. The presence of other chromophores (Fe, Cu, Zn, ...) seems to not strongly affect the colour development of the pigments, since their relative amount is low.

Acknowledgement

The work was supported by FCT (Project PTDC/CTM/72318/2006).

References

[1] E. Lopez-Navarrete, A. Caballero, V.M. Orera, F.J. Lázaro, M. Ocaña, Oxidation state and localization of chromium ions in Cr-doped cassiterite and Cr-doped malayaite, Acta Mater. 51 (2003) 2371–2381.
[2] A. Doménech, F.J. Torres, E.R. de Sola, J. Alarcón, Electrochemical detection of high oxidation state of chromium (IV and V) in chromium-doped cassiterite and tin-sphene ceramic pigmenting systems, Eur. J. Inorg. Chem. 3 (2006) 638–648.
[3] G. Costa, M.J. Ribeiro, J.A. Labrincha, M. Dondi, F. Matteucci, G. Cruciani, Malayaite ceramic pigments prepared with galvanic sludge as colouring agent, Dyes Pigments 78 (2008) 157–164.
[4] G. Cruciani, M. Dondi, M. Ardit, T. Stoyanova Lyubenova, J.B. Carda, F. Matteucci, A.L. Costa, Malayaite ceramic pigments: a combined optical spectroscopy and neutron/X-ray diffraction study, Mater. Res. Bull. 44 (2009) 1778–1785.
[5] T. Stoyanova Lyubenova, F. Matteucci, A.L. Costa, M. Dondi, M. Ocaña, J. Carda, Synthesis of Cr-doped $CaTiSiO_5$ ceramic pigments by spray drying, Mater. Res. Bull. 44 (2009) 918–924.
[6] J.B. Higgins, P.H. Ribbe, The structure of malayaite, $CaSnOSiO_4$, a tin analog of titanite, Am. Mineral. 62 (1977) 801–806.
[7] W.H. Zachariasen, The crystal structure of titanite, Z. Kristallogr. 73 (1930) 7–16.
[8] J.B. Higgins, P.H. Ribbe, The crystal chemistry and space groups of natural and synthetic titanites, Am. Mineral. 61 (1976) 878–888.
[9] M. Kunz, D. Xirouchakis, J.B. Yanbing Wang, D.H. Parise, Lindsley, Structural investigations along the join $CaTiOSiO_4$–$CaSnOSiO_4$, Schweiz. Miner. Petrog. 77 (1997) 1–11.
[10] M. Taylor, G.E. Brown, High-temperature structural study of the $P2_1/a \leftrightarrow A2/a$ phase transition in synthetic titanite $CaTiSiO_5$, Am. Mineral. 61 (1976) 435–447.
[11] R.P. Liferovich, R.H. Mitchell, Crystal chemistry of titanite-structured compounds: the $CaTi_{1-x}Zr_xOSiO_4$ ($x \leq 0.5$) series, Phys. Chem. Miner. 32 (2005) 40–51.
[12] D. Xirouchakis, M. Kunz, J.B. Parise, D.H. Lindsley, Synthesis methods and unit-cell volume of end-member titanite ($CaTiOSiO_4$), Am. Mineral. 82 (1997) 748–753.
[13] A.M. Heyns, P.M. Harden, L.C. Prinsloo, Resonance Raman study of the high-pressure phase transition in chromium-doped titanite. $CaTiOSiO_4$, J. Raman Spectrosc. 31 (2000) 837–841.
[14] M. Tiepolo, R. Oberti, R. Vannucci, Trace-element incorporation in titanite: constraints from experimentally determined solid/liquid partition coefficients, Chem. Geol. 191 (2002) 105–119.
[15] G. Monros, J. Carda, M.A. Tena, P. Escribano, J. Alarcon, Preparación de pigmentos cerámicos por métodos sol–gel = preparation of ceramic pigments by sol–gel processing, Bol. Soc. Esp. Ceram. V 29 (1990) 25–27.
[16] A. Atkinson, J. Doorbar, D.L. Segal, P.J. White, Sol–gel ceramic pigments, Key Eng. Mater. 150 (1998) 15–20.
[17] S. Eric-Antonic, L. Filipovic-Petrovic, M. Miladinovic, S. Despotovic, Sol–gel processing of ceramic pigments. Part 3. Synthesis of uvarovite, Interceram 57 (2008) 80–81.
[18] A.F. Gualtieri, Accuracy of XRPD QPA using the combined Rietveld-RIR method, J. Appl. Crystallogr. 33 (2000) 267–278.
[19] A.C. Larson, R.B. Von Dreele, General structure analysis system (GSAS), Los Alamos National Laboratory Report LAUR (2000) 86–748.
[20] CIE. Recommendations on Uniform Color Spaces: 2nd edition of Cie Publ. no. 15 (e1-1.31), Bureau Central de la CIE, Paris, 1978.
[21] V. Danek, I. Nerad, Phase diagram and structure of melts of the system CaO–TiO_2–SiO_2, Chem. Pap. 56 (2002) 241–246.
[22] K. Wisniewski, Cz. Koepke, Excited state absorption in materials containing Cr^{3+} and Cr^{4+} ions, J. Alloys Compd. 341 (2002) 349–352.
[23] M. Dondi, G. Cruciani, G. Guarini, F. Matteucci, M. Raimondo, The role of counterions (Mo, Nb, Sb, W) in Cr-, Mn-, Ni- and V-doped rutile ceramic pigments. Part 2. Colour and technological properties, Ceram. Int. 32 (2006) 393–405.
[24] M. Dondi, F. Matteucci, G. Cruciani, Zirconium titanate ceramic pigments, crystal structure, optical spectroscopy and technological properties, J. Solid State Chem. 179 (2006) 233–246.
[25] N.V. Kuleshov, V.P. Mikhailov, V.G. Scherbitsky, B.I. Minkov, T.J. Glynn, R. Sherlock, Luminescence study of Cr^{4+}-doped silicates, Opt. Mater. 4 (1995) 507–513.
[26] M. Higuchi, R.F. Geray, R. Dieckmann, D.G. Park, J.M. Burlitch, D.B. Barber, C.R. Pollock, Growth of Cr^{4+}-rich, chromium-doped forsterite single crystals by the floating zone method, J. Cryst. Growth 148 (1995) 140–147.

[27] V. Felice, B. Dussardier, J.K. Jones, G. Monnom, D.B. Ostrowsk, Chromium-doped silica optical fibres: influence of the core composition on the Cr oxidation states and crystal field, Opt. Mater. 16 (2001) 269–277.
[28] T. Murata, M. Torisaka, H. Takebe, K. Morinaga, Compositional dependence of the valency state of Cr ions in oxide glasses, J. Non-Cryst. Solids 220 (1997) 139–146.
[29] F. Matteucci, G. Cruciani, M. Dondi, G. Baldi, A. Barzanti, Crystal structural and optical properties of Cr-doped $Y_2Ti_2O_7$ and $Y_2Sn_2O_7$ pyrochlores, Acta Mater. 55 (2007) 2229–2238.
[30] M.A.U. Martines, M.R. Davolos, M.J. Júnior, D.F. de Souza, L.A.O. Nunes, Cr^{3+} and Cr^{4+} luminescence in glass ceramic silica, J. Lumin. 128 (2008) 1787–1790.